

AD-A102 900

MICHIGAN STATE UNIV EAST LANSING DEPT OF MECHANICAL --ETC F/G 20/4
AN EXPERIMENTAL STUDY OF TURBULENCE PRODUCTION MECHANISMS IN BO--ETC(U)
MAR 81 R E FALCO AFOSR-78-3703

UNCLASSIFIED

AFOSR-TR-81-0636

NL

1 - 1
AL 28-0



END

DATE

FILMED

9 81

DTIC

19 REPORT DOCUMENTATION PAGE		READ INSTRUCTIONS BEFORE COMPLETING FORM
1. AGENCY USE ONLY (Leave blank)	2. GOVT ACCESSION NO.	3. RECIPIENT'S CATALOG NUMBER
4. TITLE (and Subtitle)		5. TYPE OF REPORT & PERIOD COVERED
6. An Experimental Study of Turbulence Production Mechanisms in Boundary Layer Flows.		INTERIM <i>Sept.</i> Sep 79 - 30 Sep 80
7. AUTHOR(s)		6. PERFORMING ORG. REPORT NUMBER
Robert E. Falco		
8. PERFORMING ORGANIZATION NAME AND ADDRESS		9. CONTRACT OR GRANT NUMBER(s)
Michigan State University East Lansing, Michigan 48824		AFOSR-78-3703
10. CONTROLLING OFFICE NAME AND ADDRESS		10. PROGRAM ELEMENT PROJECT, TASK AREA & WORK UNIT NUMBERS
AFOSR/NA Bolling A.F.B., D.C. 20332		61102 F 2317/42 T A2
11. CONTROLLING OFFICE NAME AND ADDRESS		12. REPORT DATE
AFOSR/NA Bolling A.F.B., D.C. 20332		27 Mar 81
13. CONTROLLING OFFICE NAME AND ADDRESS		13. NUMBER OF PAGES
AFOSR/NA Bolling A.F.B., D.C. 20332		26
14. CONTROLLING OFFICE NAME AND ADDRESS		15. SECURITY CLASS (of this report)
AFOSR/NA Bolling A.F.B., D.C. 20332		Unclassified
15. CONTROLLING OFFICE NAME AND ADDRESS		15a. DECLASSIFICATION DOWNGRADING SCHEDULE
15. CONTROLLING OFFICE NAME AND ADDRESS		
16. DISTRIBUTION STATEMENT (of this Report)		
Approved for public release; distribution unlimited.		
17. DISTRIBUTION STATEMENT (of the abstract entered in Block 20, if different from Report)		
DTIC AUG 17 1981		
18. SUPPLEMENTARY NOTES		
19. KEY WORDS (Continue on reverse side if necessary and identify by block number)		
Turbulence, production, vortices, transfer, bursting		
20. ABSTRACT (Continue on reverse side if necessary and identify by block number)		
The mechanism of turbulence production is identified. Simultaneous flow visualization and hot-wire anemometry have been used. A new scaling of the burst rate has been found.		

AD A102900

DTIC FILE COPY

INTERIM REPORT

~~AFOSR Grant 78-3703~~

AFOSR-78-3703

**"AN EXPERIMENTAL STUDY OF TURBULENCE PRODUCTION MECHANISMS
IN BOUNDARY LAYER FLOWS"**

October 1, 1979 to September 30, 1980

R.E. Falco
Department of Mechanical Engineering
Michigan State University
East Lansing, MI 48824

SUMMARY OF PROGRESS

We have achieved a number of our proposed goals, which are reiterated below.

1. To develop a state of the art digital data acquisition system which can simultaneously digitize 16 channels of data and a timing signal from simultaneous high speed movies.
2. Develop visualization techniques which give us three-dimensional information about the coherent motions under investigation, and which can be used with simultaneous hot-wire anemometry.
3. Obtain length scales of the pocket flow module and compare them to the streaky structure scales as well as the scales of the vortex ring-like Typical Eddies of the outer region.
4. Determine whether the pocket flow modules (which previously had been observed to create the largest transfer of any event in the wall region) occurred as frequently as the bursts found by Kline and others.
5. Determine whether the passage of a pocket flow module resulted in the hot-wire information found by other investigators to be characteristic of the bursting process.

81 8 14 087

**Approved for public release;
distribution unlimited.**

6. To obtain simultaneous visual and hot-wire information about the interaction of the outer region with the wall which produces the pocket flow modules.
7. To determine the accuracy of the vortex ring/wall interaction model of the pocket flow module.

We have met goals 1-5, although as of September 30, our data acquisition system was not operating due to an unfortunate accident. Information obtained during this year has indicated that goals 6 and 7 will require more study. Figures 1 through 7 as well as AIAA Paper 80-1356 summarize the results obtained.

Figure 1 shows the rate of occurrence of pockets compared to the burst rate found in the Stanford studies. Both the overall frequency of occurrence of pockets, and the frequency of occurrence of pockets during their ejection phase, is shown. We see that the correspondence between the occurrence of pockets ejecting sublayer fluid and the ejections found in the Stanford studies is excellent. Furthermore, we see that pockets are observed approximately four times as often, thus three out of four times that pockets pass our measurement station they are not in their ejection phase. The data has been scaled using wall layer variables, which remove the Reynolds number dependence significantly better than outer layer variables. This suggests that the large scale motions (proportional to the boundary layer thickness) which scale on U_{∞} and δ , do not control the bursting process as had been previously thought.

Figure 2 shows the ratio of the pocket flow module cross-stream dimension to the streaky structure (Stanford studies and others) spacing, both measured in our wind tunnel over approximately a decade in Reynolds

Accession for	
DTIC GRA&	<input checked="" type="checkbox"/>
DTIC TIR	<input type="checkbox"/>
Unannounced	<input type="checkbox"/>
Justification	<input type="checkbox"/>
By	
Distribution/	Availability Codes
Dist	Avail and/or
	Special

number. We see that the pockets scale exactly as the overall streaky structure. This reinforced our earlier observation (Falco, Sixth Biennial Symposium on Turbulence, Rolla, 1979), that the streaky structure was the result of pockets forming both singly and in groups.

Figure 3 shows the ratio of the vortex ring-like Typical Eddies, which form away from the wall, to the overall streaky structure spacing. We can only conveniently measure the streamwise and normal Typical Eddy scales, but the spanwise scale falls in between these two. We can again see that there is a remarkable correspondence in scales, especially considering that the measurements extend over a decade of Reynolds number. This suggests that Typical Eddies might very well be associated with the formation of pockets, and therefore with the streaky structure.

Figure 4 shows that the Typical Eddies are approximately equal in size to the Taylor microscale. Thus we see that if Typical Eddies are producing the pockets, the pockets are produced by microscale motions, not the large eddies of the boundary layer. This possibility is consistent with the scaling found for the time between pockets (figure 1).

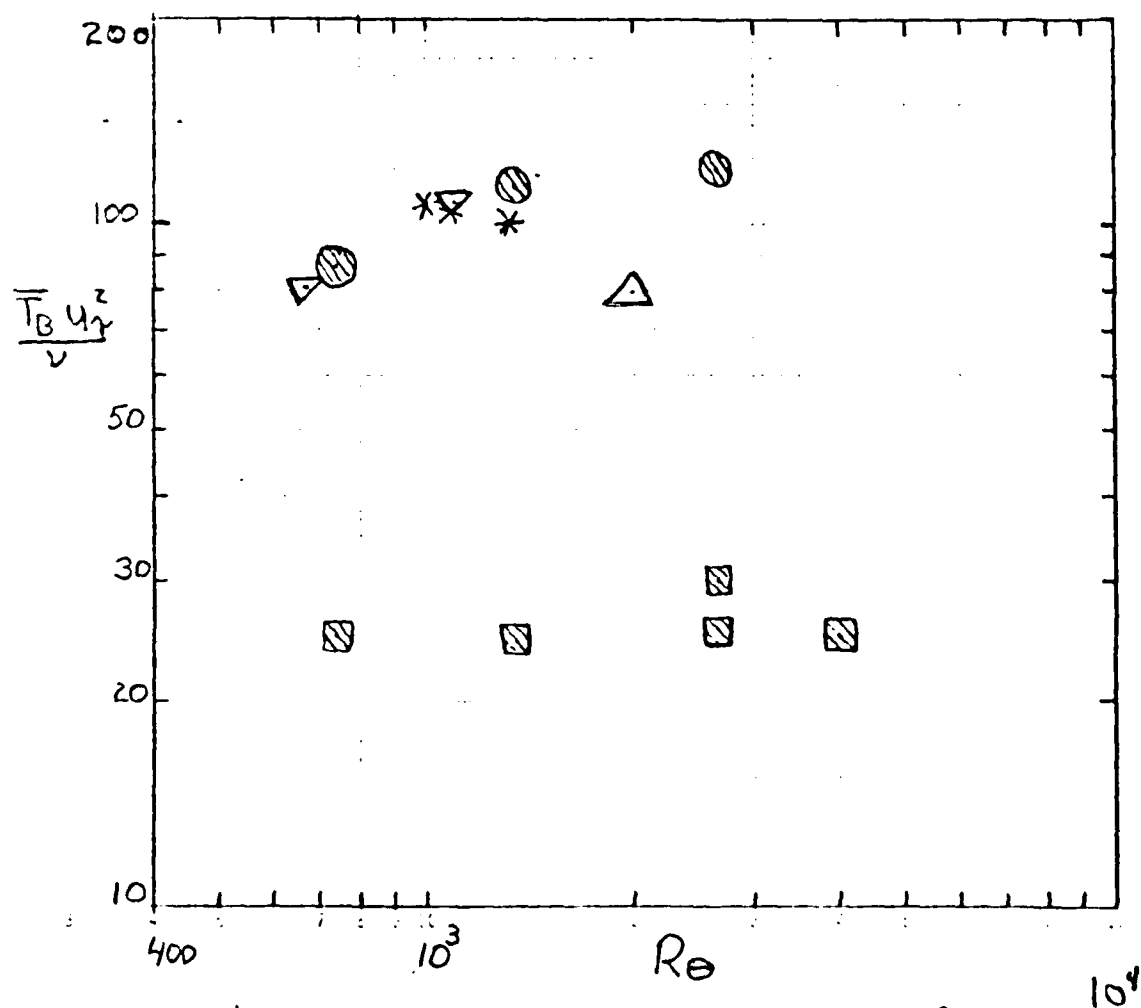
Goal number 5 has been attained as described in AIAA Paper 80-1356 (enclosed). In summary, we have found that the pocket flow module evolves through a series of five stages. Each of these stages exhibits an event which has been the subject of study of other investigators. Thus, strong sweeps, streamwise lift-up and oscillation, the formation of sharp shear layers, ejection and breakup events are all part of the pocket flow module's evolution!

Figure 5 shows a comparison of the data from the Blackwelder and Kaplan's burst detection scheme and the $\langle uv \rangle$ signatures from the pockets during stages three and four. Considering that the techniques of condi-

tional sampling are entirely different, the correspondence is quite good. It suggests that their "vita" technique picks up the sharp shear layer that forms during stages three and four of the pocket evolution. If this is true, then their explanation of the origin of the ejection as due to this shear layer becoming unstable would not be correct, since we are in the middle of the pocket flow module evolution. Furthermore, it is clear from figure 4 of the AIAA paper, that although some of the Reynolds stress is detected by the "vita" technique, a large fraction is not.

Figure 6 shows a photo of a vortex ring-like Typical Eddy approaching the wall. The top of the ring is approximately $100 y^+$. Flow is from right to left. We are currently attempting to obtain laser sheet side views of this quality with simultaneous plan views showing the pocket patterns (see figure 1 of the AIAA paper), along with four or possibly eight wire probes to allow us to determine the nature of the interaction of naturally created vortex rings with the wall layer flow in the fully turbulent boundary layer. To help us understand, and to make us aware to look for details of this interaction, we are concurrently studying the interaction of an artificially generated vortex ring with a wall. This model flow field not only exhibits all of the features discussed above, but in addition explicitly shows the role of vortices in the formation of the pocket pattern, in the streamwise lift-up of wall layer fluid, and in the ejection of fluid from the downstream portion of the pocket. We hope to be able to examine the detailed role that vortices play in the evolution of the pockets found in real turbulent boundary layers in the near future.

- Pockets (Stage III and IV)
- ▣ Pockets (all Stages of development)
- * Ejections (Schraub and Kline)
- ▽ Ejections (Kim, Kline Reynolds)
- △ Ejections (Runstadler, Kline, Reynolds)



Average time between ejections scaled
on wall region variables.

Figure 1

Pocket Width / Streak Spacing

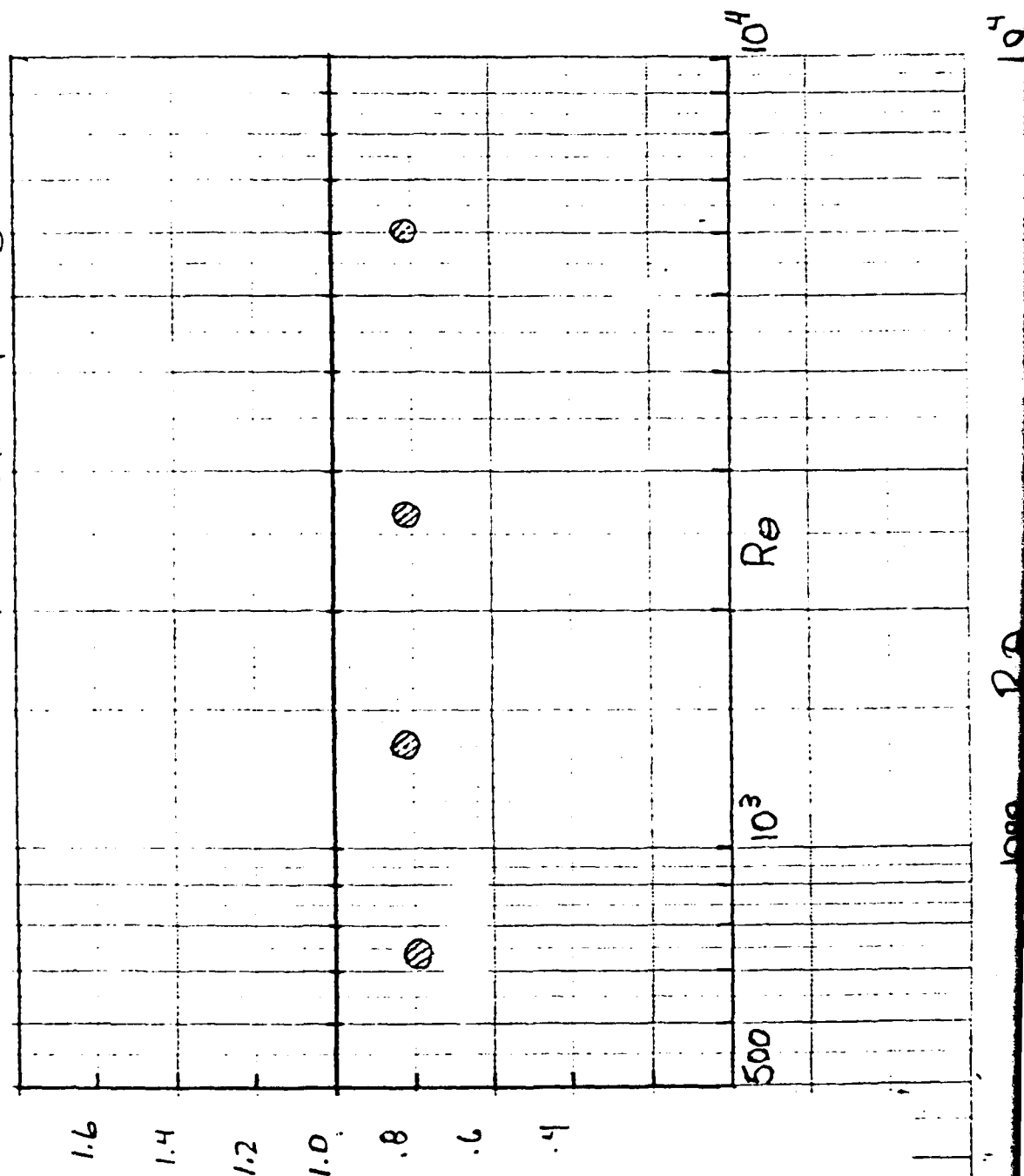
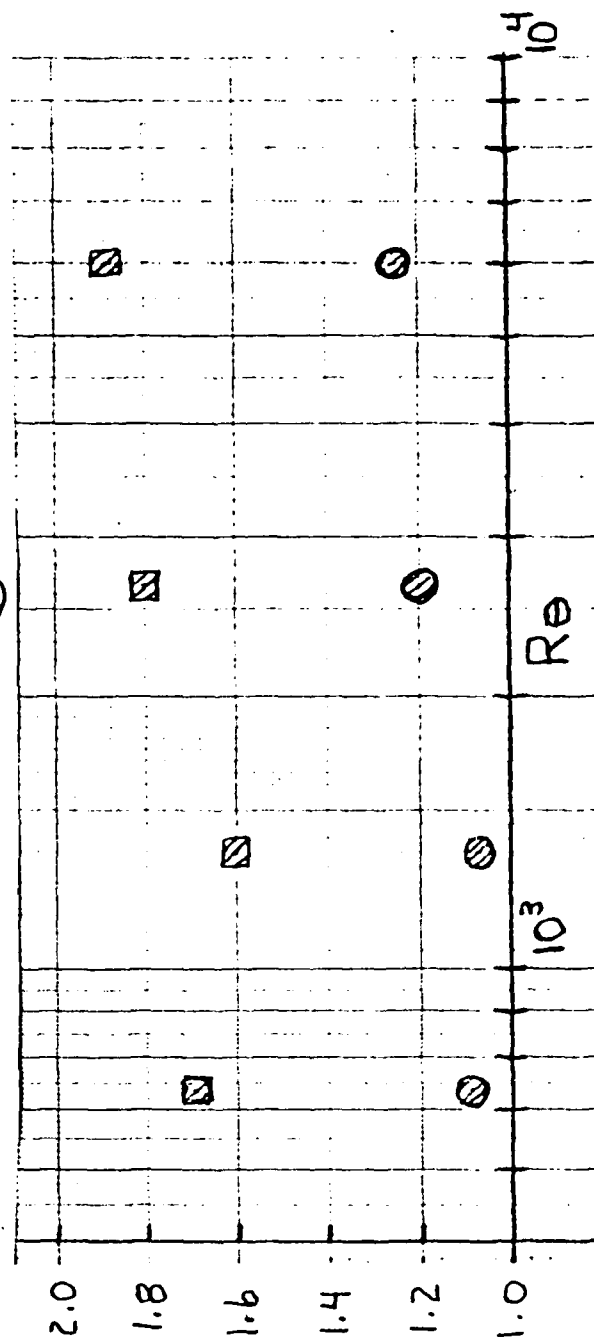


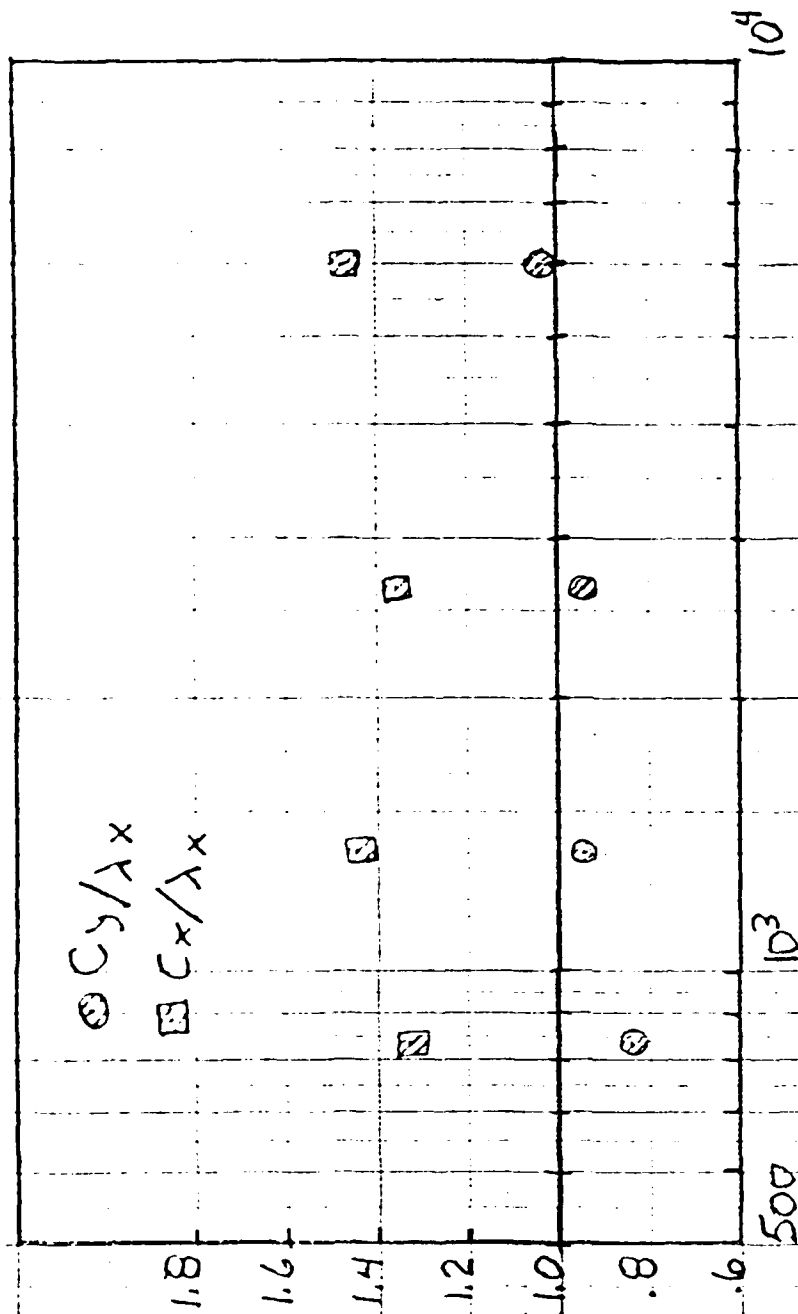
Figure 2

○ Cy/Streak Spacing
 □ Cx/Streak Spacing



Ratio of Typical Eddy Scales to the
 Overall Streaky Structure

Figure 3



RATIO OF TYPICAL EDDY SCALES TO
TAYLOR MICROSCALE

Figure 4

1000 R_D

10⁴

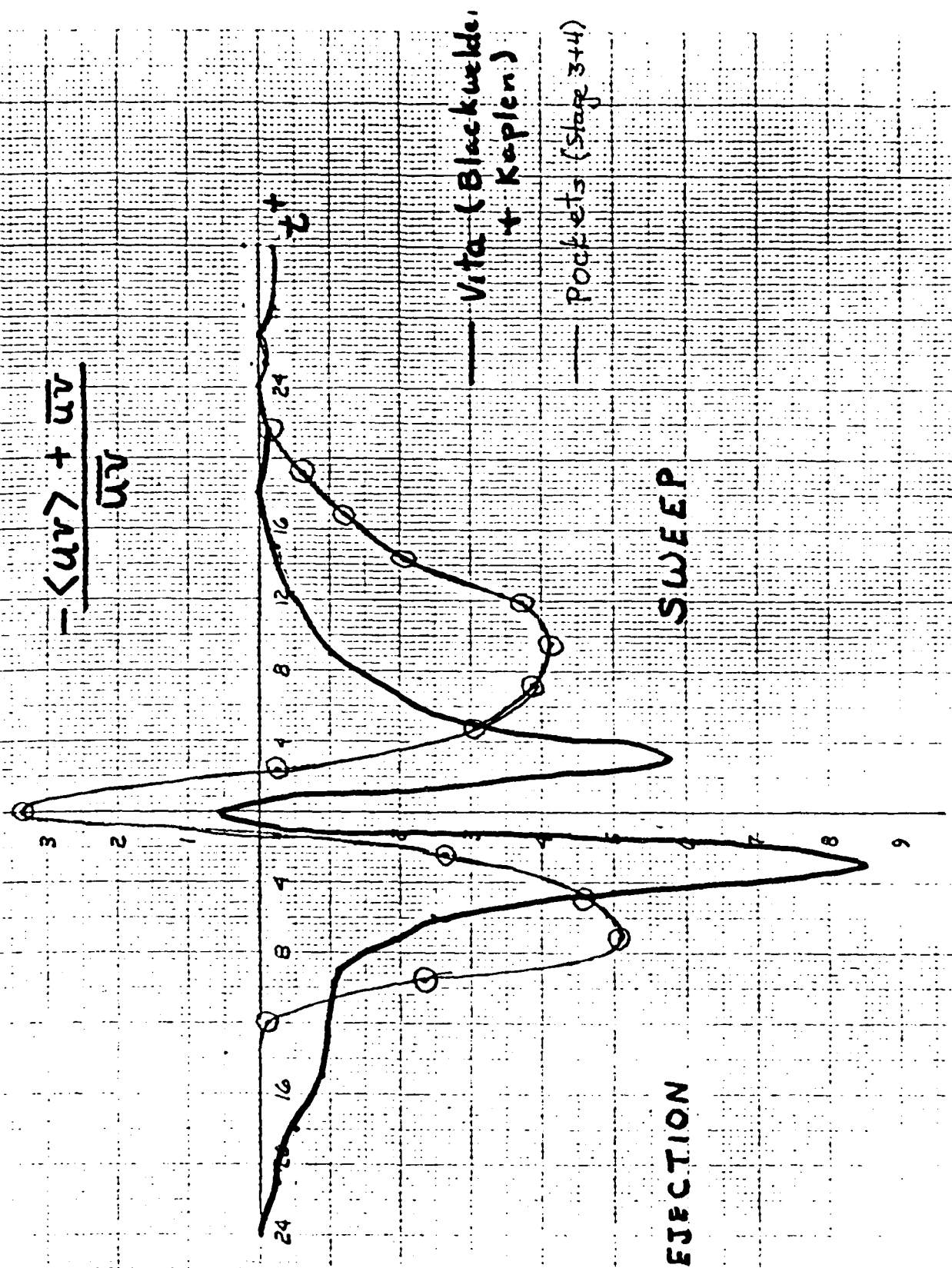
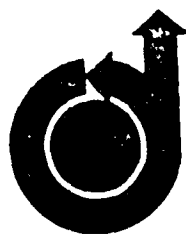




Figure 6



AIAA-80-1356

**The Production of Turbulence
Near a Wall**

**R. Falco, Michigan State
University, East Lansing, Mich.**

**AIAA 13th
FLUID & PLASMA DYNAMICS
CONFERENCE**

July 14-16, 1980/Snowmass, Colorado

For permission to copy or republish, contact the American Institute of Aeronautics and Astronautics-1290 Avenue of the Americas, New York, N.Y. 10019

THE PRODUCTION OF TURBULENCE NEAR A WALL

M. E. Falco
Department of Mechanical Engineering
Michigan State University
East Lansing, MI. 48824

Abstract

Simultaneous visual and hot-wire anemometer measurements of the flow in the wall region of turbulent boundary layers have revealed a close connection between local repetitive visual patterns seen in the sublayer in plan view; wallward moving high speed fluid (sweeps), and ejections of sublayer fluid, seen in side views; and periods of important perturbations in the variables u , v , uv , du/dy , du/dx , and dv/dx near the region of maximum turbulence production. Our interpretation of the data indicates that the turbulence production process is initiated when a three-dimensional vortical sweep, of scale the $O(100)$ wall layer units, interacts with the wall, and that it is completely describable in terms of the evolution of the resulting three-dimensional vortical sweep/wall interaction. It is shown that this flow module contains the features of the turbulence production mechanism that have been observed by many investigators.

1. Introduction

The search for mechanisms responsible for the production of turbulence near a wall has resulted in a large number of semi-empirical models. Some of these explicitly model the longer time scale events, and infer that rapid breakdown of the wall region flow will ensue as a result of the modifications these motions make to the mean velocity profile, while others are principally concerned with detailing the period during which the rapid changes occur. Models of the first kind have been put forth by Townsend,¹ Bakewell and Lumley,² Lee, Eckelman and Hanratty,³ and others. These consist principally of streamwise orientated vortices which are attached to the wall. From space-time correlation measurements, Bakewell and Lumley found little fall-off of the correlation of streamwise velocity (u) over 40 viscous lengths, suggesting that the vortices are well correlated over this length. Some authors have hypothesized that the vortices extend the order of $x^+ = 1000$ ($x^+ = xu^*/\nu$), which corresponds to the order of the longest streaks found in wall region visualizations. Recent probe measurements of Blackwelder and Eckelmann⁴ have confirmed the existence of streamwise vorticity in the sublayer, and suggest that it occurs in counterrotating vortex pairs, but they were unable to measure the length of the vortices.

Models which are concerned with the details of the rapid breakdown of sublayer fluid documented by Kline, and co-workers

at Stanford University,^{5,6,7,8} Corino and Brodkey,⁹ Grass,¹⁰ and others, have hypothesized many different mechanisms to describe the events. These include instability of the instantaneously inflected velocity profile,^{2,7,11} separation of the wall layers resulting from local adverse pressure gradients,⁶ formation of sharp shear layers which become unstable,¹² inflows and continuity,^{13,14} wave focusing,¹⁵ vortex induced lift-up of wall layer fluid,^{16,17,18,19} vortex-wall instabilities,²⁰ and vortex ring/wall interactions.²¹

It is possible, by ignoring the many detailed differences in these models, to classify them as models which start with concentrated vorticity, and describe the results of stretching of this vorticity on the wall region flow, or models which start with the formation of a shear layer in the wall region, the breakdown of which results in the ejection of fluid into the outer region. An exception is the model of Ref. 14, which relies solely upon continuity.

bounds on the time scales, and a pretty accurate estimate of the velocity scale of the wall region events have been established. Practically all of the interesting events in the wall layers take place in $t^+ = tu^*/\nu$ of less than 30, and that within this period, high shear layers develop, intense uv contributions due to high speed fluid moving towards the wall occur (sweeps), as well as intense uv contributions due to fluid moving away from the wall (ejections), and pressure peaks of both positive and negative sign. Furthermore, both space-time correlation estimates and measurements of the passage of either a visual impression (such as a pocket), or a pressure pulse, indicate that the convection velocity is approximately $0.6U_{\infty}$. An important point for both of these quantities is that there does not appear to be a significant Reynolds number dependence. Thus it is possible to convert from time scales to length scales for the purposes of comparison, with relative confidence.

The foregoing information suggests that visualization of the wall region should reveal disturbances with a length scale the order of $l^+ = (t^+) u_c / \nu < 100$, for bursts, or sweeps, or low pressure pulses, or high shear layers. Combining this fact with the spanwise scale of wall layer events (Ref. 3,5,6) which is approximately $z^+ = 100$, it is expected that "local" three-dimensional features will mark the bursting process. Falco²² first reported visual indications of the appearance of coherent, repetitive disturbances of this scale in the sublayer of a turbulent boundary layer, which occurred at random positions with respect to the longer streaky structure (see Ref. 5,6,7,8). The technique used was to fill the boundary layer with oil fog

contaminant, and then allow it to wash out. A sheet of laser light illuminated the region from $y^+ = 9$ to 14 . After some time, a condition existed in which, on average, there was smoke between the laser sheet and the wall, but clear fluid above. During this period we could see regions of clear fluid of the scales mentioned above forming in the light sheet. Because of their appearance and small scale, we called the regions "pockets". It has turned out that the pocket patterns are more clearly seen using the flow visualization technique, used extensively at Stanford, of ooze marker into the sublayer through a slit in the wall. Figure 1 shows two photos of the sublayer. The pocket patterns are clearly seen. The exact shape depends upon the stage of evolution of the pockets as discussed below. The average scale of these patterns is the order of $x^+ \approx 100$, $z^+ \approx 100$ (Falco²⁰), and their average convection velocity is approximately the same as reported for other indications of important wall region events. Thus, the pocket pattern appears to be associated with the bursting process. It was unexpected, however, to find that pockets appeared both when the long streaky structure broke up (Stanford references), as well as in between the long streaks.

We intend to show that the pocket pattern is, in fact, the footprint of the turbulence production process that has been identified in the above mentioned investigations, and that the pocket flow module incorporates both the sweep and ejection events as well as the formation of an intense shear layer.

II. Experimental Techniques

Experiments were conducted in a continuously running boundary layer flow visualization tunnel. The flow was made visible by contaminating it with tiny oil droplets. This marked fluid has been visualized with both flood lighting, and laser light which was expanded into a sheet. Details of both the tunnel and flow visualization technique are described in Ref. 25. For the present experiments, two additional techniques have been used to visualize the flow. The oil fog "wash out" technique, mentioned in the introduction, is a technique which allows a quasi-uniform concentration of marker to be present in the wall region over several boundary layer thicknesses, without problems associated with marker introduction. This was used together with one or more sheets of laser light, which could be placed where desired. The other was the smoke slit technique. A specially designed slit, which introduced oil-fog at 9 degrees to the oncoming flow, across a 30 cm line, was combined with flood light illumination, to obtain an alternative view of the pockets, and get better information about lift-ups.

Hot-wires were placed in the flow in several of the experiments. Details of the

probes, calibration techniques, and data acquisition, are described in Ref. 23 and 25. Briefly, the system allowed simultaneous sampling of all the wires. The most used probe arrangement consisted of 4 wires, two arranged in an x and two parallel to each other, so that u , v , uv , and du/dy could be directly obtained, and du/dx and dv/dx inferred using a local Taylor hypothesis. Combining dv/dx and du/dy , ω_z was obtained. At $R_\theta = 1066$, the parallel wires and the x-wires were separated by $y^+ = 3.6$. Additional details are given later.

III. Results

It is important to distinguish, at the outset, the difference between the visual pocket pattern imposed on the marker in the wall region, and the signatures resulting from the flow at various probe positions within, to the side of, and above the pattern. If we assume that some flow module is responsible for the pocket pattern in the wall layers, then the signals and visual pattern must show a strong correlation, but will not, in general, show a one to one correspondence. Falco²⁴ has found that in the case of pocket patterns that formed within a laminar boundary layer that was perturbed by a turbulent wake, the hot-wire signals indicated the occurrence of significant perturbations both within the visually defined boundaries of the pocket pattern, as well as within approximately one pocket length downstream of the pattern. In this case, both hot-wire and visual signals indicated that a flow module was approaching the wall. It produced the pocket pattern as well as the perturbations just downstream of the pocket pattern. Based upon this information, we will call the entire sequence of events that is associated with the formation and evolution of the visual impression, and of the hot-wire signals in the wall region which are associated with the pattern the "pocket flow module".

It is important to determine the rate at which the pocket pattern passed a fixed point, and to compare this with the measured burst rate obtained by a number of investigators. In order to compare information, we had to count pockets that were resulting in the lift-up of wall layer fluid as they crossed the observation point. From our experience with pockets (see Ref. 23,24), we knew that the majority of the lift-ups occurred after the pocket reached its "fully developed" state. This stage in the pocket evolution is characterized by the development of a pointed appearance of its upstream boundary (details are given below). Counting only fully developed pockets, the number of pockets per second, non-dimensionalized by the free stream velocity and the boundary layer thickness at $R_\theta = 1355$, is approximately 5. Table 1 compares this value with others found in turbulent boundary layers. It is concluded that

pocket flow modules must be associated with the bursting process. Furthermore, it is worth noting that if pockets were counted without regard to their stage of evolution, the rate of occurrence increases considerably.

Inspection of the combined simultaneous visualized wall layer flow and hot-wire measurements, have shown a high correlation between the evolution of the pockets in which there is a rapid evolution of the marker, and the periods of high instantaneous Reynolds stress, high shear and/or vorticity. The picture is, however, complicated, due to the rapid evolution and change in the phasing of these quantities. It has been found that all four of the possible motions that can contribute to Reynolds stress are associated with the pocket flow module at different times in its evolution. These four events have been called ejections ($u(-)$, $v(+)$), sweeps ($u(+)$, $v(-)$), inward interactions ($u(+)$, $v(-)$), and outward interactions ($u(+)$, $v(+)$), see Wallace et al.²⁰ It is thus necessary to examine signatures at specific times after formation of a pocket pattern to uncover the fact that a highly coherent evolution takes place. Measurements of the lifetimes of pockets have shown that they persist for the order of $t^+ = 30$. However, they evolve continually over this time period. Experience has shown that the signal response can change significantly in $t^+ = 4$, which is short compared to the time of passage of the pocket flow module over a wire, which depending upon the stage of evolution, ranges from $t^+ = 10-30$. This fact, combined with the difficulty in determining the moment of formation of a pocket, has made the process of accumulating ensemble averages of the pocket signatures at various representative intervals in the evolution of the flow module a prolonged task. Thus, the results presented herein will be qualitatively representative of the evolution. Work is in progress to more accurately measure pocket inception and to build sufficiently large ensembles, however, the nature of the turbulence production mechanism can be clearly shown with the present information.

Fig. 2 shows simultaneous records of uv , du/dx , dv/dx , du/dy , v , and u , for δ boundary layer thicknesses. The boundary layer conditions are: $R_0 = 1060$, $u^* = .101$ ft/sec $\delta = 5$ in, $y^+ = 16$. We can see that there are two regions where significant uv contributions occur, if we compare the signals with the long time average value of uv , $-.014$ ft²/sec. We have inspected records such as these covering 207 δ . From this sample we confirmed that these peaks are representative of instances of large uv . They are respectively 6.4 and 10 times the average uv . The recent work of Comte-Bellot et al.²⁷ also suggests that these peaks are significantly higher than their quadrant breakdown discrimination technique requires. Our simultaneous visual

measurements have shown that both of these peaks have resulted from the passage of pockets. The time for passage of the earlier evolving pocket flow module was $t^+ = 23$, while the later pocket required $t^+ = 26$ to pass over the wire. These times are indicated by vertical dotted lines in the figure. Although both signatures resulted from the passage of pockets, they are significantly different in content. The earlier signature contributes its largest uv as the result of upward moving low speed fluid, i.e. An ejection, whereas the later signal contributes its largest uv due to wallward moving high speed fluid, i.e., a sweep. The age of the two pockets was $t^+ = 16$ and $t^+ = 12$ respectively. Inspection of the remainder of the data record revealed that a very high correlation existed between significant perturbations in the uv , du/dx and dv/dx and du/dy signals, and the passage of the visual pocket pattern. Signals such as those in Fig. 2 suggested that the signatures were evolving in a consistent manner as the pocket evolved, and that the evolution involved creation of both ejections and sweeps as well as the other interactions and the formation of intense shear layers.

An example of the strong correspondence between the pocket and the signal perturbations is exemplified by the velocity gradient du/dy . The number of du/dy peaks which were greater than $2\langle du/dy \rangle$ was first found. There were 47 of them. Then the movies were examined to determine what percentage of these peaks was attributable to pockets. It was found that 45 were, an astonishing 96 per cent. We then determined the age of the pockets that were associated with the high peaks. The result is shown in Fig. 3. It can be seen that pockets had to be at least $t^+ = 6$ old before being able to produce a shear layer of this magnitude, and that pockets older than about $t^+ = 30$ rarely contained such a high shear layer. The average age of pockets contributing $du/dy > 2\langle du/dy \rangle$ was $t^+ = 10$. Vorticity peaks at $2\langle du/dy \rangle$ were of duration $t^+ = 3$ with a standard deviation of $t^+ = 1.7$. Pockets which were younger than $t^+ = 6$ were found to exhibit a different du/dy signature. In general they were associated with values of du/dy which were lower than the mean value.

Further progress in understanding the pocket evolution requires a breakdown of the evolution into stages, each characterized by the dominance of one of the Reynolds stress producing events. The data indicated that it was possible to come close to achieving this goal, by identifying five stages in the evolution of the pocket flow module. We will now discuss these five stages paying special attention to the uv , du/dy , and u signatures, and the visual impression of the pocket from its inception. Fig. 4 shows these three signatures and the visualized pocket pattern for each of the five stages. The stages differ somewhat in duration. Stages

one through three have a duration of approximately $t^+ = 8$. Stage four had a duration of $t^+ = 12$, and stage five was approximately the same duration. There was an overlap of approximately $t^+ = 4$ from the measured time of pocket pattern formation, to a given stage. The variation in the signals, the fact that rapid evolution occurs in $t^+ = 4$, and the uncertainty of the inception instant all combined to limit our resolution. It should be noted that the data was digitized at a rate of 10 points per t^+ , so that the resolution problems were confined to the visual measurements. The signatures are "eyeball" ensemble averages of the signals from 10, 7, 6, 9 and 17 occurrences of stages one through five respectively. Because of the considerable coherence of the evolution, the qualitative features of the stages are adequately represented by samples of this size. An attempt has been made to indicate approximate non-dimensional magnitudes of the signals and to draw the temporal extent so as to approximately scale with the visual impression. In all cases, only pockets which essentially centered themselves along the probe path were used. This criteria was applied loosely, because of the obvious difficulties, but enough observations of pockets in the relevant stages which were not very well centered were made to add qualitative confidence to the discussion which follows.

We begin with stage one, which includes pockets that intersect the wire anywhere from their inception, to $t^+ = 8$ afterwards. The visual impression in either the laser sheet illuminated buffer layer, or in the sheet of marker oozed out of a slit in the wall, is of a roundish hole being created in the smoke-marked wall region. It appears as if the marker has been pushed out of the way by a wallward moving disturbance. The streamwise velocity is high over the entire hole, and the uv signal is the order of $10\langle uv \rangle$. The highest uv signals of the entire record were found during this stage of evolution of the pocket flow module. The shear du/dy is less than the long time average. Thus we can conclude that pockets are formed by sweeps which come to the wall. It is worth remarking that we would not in general expect the low value of du/dy , since both the flow models of Ref. 12 and Ref. 13 suggest that incoming high speed fluid results in a high shear at its interface as it approaches the wall. Furthermore, in only 1 out of the 16 stage one pocket events, was du/dx significant. Taken together, the absence of both of these shears argues against the hypothesis that incoming higher speed fluid results in an intense, sharp shear layer. We will return to this point later.

Stage two is characterized by the formation of the characteristic crescent shape (see Fig. 4), between $t^+ = 4$ and $t^+ = 12$. Flow visualization at this stage

indicates the lift-up of sublayer fluid and its rotation about a vortex which is apparently formed or amplified along the boundary of the crescent shaped pocket (Falco²³). Both laser sheet visualization and sublayer slit visualization (using flood lighting) show this lift-up of sublayer fluid, and its rapid return back to the wall. This rotation has the same sign as the vorticity of the mean flow at the upstream end of the pocket. The vortex however, follows the contours of the crescent, and thus has a streamwise orientated portion. The streamwise velocity signal during this stage continues to indicate that high speed fluid is in the pocket. The uv signal remains strongly negative, indicating the continued presence of the sweep. However, a dramatic change has occurred in the du/dy signal. It has become strongly positive near the upstream end of the pocket pattern. This result supports the visual observations mentioned above (also see Ref. 23), that a vortex has formed, or that vorticity has been amplified along the pocket boundary. Furthermore, du/dx remains small, indicating that the flow within the pocket is not an inclined shear layer. This gives additional support to the picture of a vortex at the boundary.

Stage three occurs in pockets that are between $t^+ = 8$ and 16 old. The pocket pattern becomes pointed at its upstream end, and elongated. The lifting up of sublayer fluid continues, but is primarily observed to happen along the sides of the pocket as indicated in Fig. 4. The streamwise velocity perturbation begins to show the formation of a region of low velocity forming a little bit downstream of the pocket pattern, however, within the boundaries of the pocket high speed fluid continues to move towards the wall maintaining the large uv contribution. The uv signature shows that just downstream of the pocket pattern an ejection is developing. At the downstream boundary uv is positive, indicating the high speed fluid is moving away from the wall (an outward interaction). The velocity gradient du/dy continues to change appreciably. Just downstream of the pocket pattern, it has become significantly positive. At the downstream pocket boundary, du/dy has become significantly lower than the mean shear. Upstream, within the boundary of the pocket pattern it remains positive, but is reduced in magnitude from the values it had in stage two. We have also inspected dv/dx at this stage. It is in general much smaller than du/dy , and only occasionally becomes significant. During stage three, however, dv/dx shows a significant positive value during the time du/dy is negative (lower than the mean shear). This suggests the presence of vorticity of sign opposite to the mean vorticity of the layer is present at the downstream boundary of the pocket at this stage.

Stage four occurs when the pocket is between 12 and 14 t^* (13). The visual impression indicates a steepening upstream portion and apparent rapid movements toward the downstream end, which are sometimes accompanied by vortices, and sometimes by a buildup of smoke near the front of the pocket pattern, indicating a more intense and concentrated lifting of sublayer fluid than previously observed at the upstream end or along the sides. Visual results using two mutually orthogonal sheets of laser light, one in the buffer layer, and one perpendicular to the flow, have shown that a discrete vortex is rapidly lifted up from the wall region. Fig. 5 shows this event occurring. The top half of the photo shows the wall region structure. One of the pockets is roughly centered over the vertical light sheet which produces the lower half of the picture. In the side view (lower half) at the downstream end of the pocket pattern, we see a vortex which is moving away from the wall. An indication of fluid rotating in the opposite direction immediately behind this vortex is also apparent. The streamwise velocity perturbation shows that the region of velocity defect which formed in stage three has increased in intensity, while the region of velocity excess, still contained within the pocket boundary, has only slightly diminished. The uv signature, on the other hand, indicates that the region of defect is associated with a significantly strengthened ejection. At the downstream boundary of the pocket, uv is positive; the outward interaction continues at about the same strength as it had during stage three. Within the boundary of the pocket outline, the sweep also continues, but at a significantly reduced intensity, which considering the fact that the velocity excess is still relatively large, suggests that the high speed fluid has begun to move more parallel to the wall (this may be the cleansing sweep noted by Corino and Brodkey). The velocity gradient du/dy continues to undergo significant changes. Just downstream of the boundary of the pocket pattern, the gradient increases by a factor of three. The width of this peak, the largest du/dy magnitude found in the boundary layer at this level, is the order of $t^* = 3$. The du/dy peak which formerly existed within the pocket pattern during stage three and earlier, has disappeared. Examination of the gradient du/dx , shows that it also attains its maximum values during this stage of the pocket's evolution, which also is the maximum du/dx found in the boundary layer at $y^* = 16$. The average duration of this peak about its zero value is $t^* = 6.7$. Examination of dv/dx indicates that it is, on average, close to zero at the downstream boundary of the pocket pattern, unlike the significant positive value which existed during stage three. The overall impression is that, at stage four a strong shear layer develops at the downstream end of the pocket impression, and that strong ejection of sublayer fluid is occurring immediately

downstream of this shear layer. This picture has been previously arrived at by Eckelmann et al.¹³ and by Blackwelder.¹² We now see where it fits in the overall production process (we will return to these comparisons later).

Stage five occurs between $t^* = 20$ and $t^* = 30$, approximately. By this time the visual impression of the pocket pattern has become distorted, but some evidence of its presence is usually detectable. The impression of intensive mixing at the downstream end is sometimes apparent in experiments which visualized only the sublayer or buffer layer. In the experiments with simultaneous plan and side views, we can see an orderly ejection, described during stage four, suddenly become chaotic, with all indications of vortices and/or any other sense of coherence disappearing. This doesn't always happen during the ejection. Sometimes the vortices can be seen to continue further out, and evolve substantially. But these occurrences were rarely observed compared to those which involved breakup between $y^* = 30-50$. Looking at the signals, we see that the streamwise velocity reaches its minimum value, and is negative both downstream and within the pocket pattern. The high speed region within the boundary of the pockets has disappeared. The uv signature shows an intense ejection, i.e., the order of $7\langle uv \rangle$ (note that the intensity of sweeps in stages one through three is a little higher, the order of $8-10\langle uv \rangle$). These ejections are the most intense observed in the entire record. In 55 per cent of the sample, a small positive uv contribution was noted at the end of the ejection interval, which was due to inward moving fluid of low speed. The velocity gradient du/dy is significantly below the mean shear of the layer suggesting that either the ejecting fluid has fluctuating vorticity of opposite sign from the mean vorticity of the layer during its breakup, or that the breakup results in a well mixed region of low and high speed fluid. Further inspection indicated that near the upstream end of many of the ejection intervals, du/dy became slightly positive. The gradient du/dx consistently showed that the fluid first accelerated and then decelerated as the ejection passed over the probe. The gradient dv/dx was essentially zero throughout stage five. The overall impression gained from this stage is that a large scale, well mixed region of fluid is ejecting away from the wall near the downstream end of the pocket pattern. The absence of significant values of du/dx or dv/dx suggests the "well mixed" description, as does the negative du/dy found during the breakup. The negative fluctuating du/dy may also suggest that the overall breakup motion has fluctuating vorticity of opposite sign from that of the mean flow.

IV. Model of Production Process

The sequence of events described above involved all of the four Reynolds stress producing events; sweeps, ejections, outward interactions and inward interactions. It begins with high speed fluid moving towards the wall. As noted by Lighthill¹⁰ whether this fluid is irrotational or rotational it will result in the production of vorticity on the wall around the stagnation point it creates. On the downstream side of the sweep, this vorticity will have the same sign as the mean vorticity of the boundary layer, but on the upstream side it will be of opposite sign. As this newly created vorticity passes the probe during stage one, we should see an increase in du/dy due to it, but we don't. Instead, we have a decrease in du/dy . This can only be explained if the sweep has vorticity of opposite sign from the mean vorticity of the layer, at its downstream end. If this vorticity was strong enough the net effect could be a decrease in du/dy . This possibility is supported by the fact that du/dx is not significant because, taken together, the facts indicate that the sweep does not appear to create a shear layer at its downstream boundary.

If vorticity of opposite sign exists at the front of the sweep, which creates the three-dimensional pocket pattern, it is reasonable to expect that these vortex lines close upon themselves at the upstream end of the three-dimensional sweep. The events of stage two support this suggestion when the pocket flow module passes during stage two, we find a sharp increase in du/dy near the upstream end of the pocket pattern, and visual observations show that sublayer fluid is lifted-up from the wall, rotates around a vortex core which has the same sign as the mean vorticity of the layer, and returns to the wall. This is the motion we would expect if the sweep were a vortex ring. It is the opposite of what we would expect from the vorticity generated by wallward moving irrotational fluid which created a stagnation point flow.

However, even a vortex ring moving towards the wall creates a stagnation point, and generates vorticity as indicated in Ref. 10. Thus at the upstream end of the pocket flow module, vorticity of opposite sign from that of the mean vorticity of the layer is being created. The fact that the net vorticity shows a strong increase above the mean value indicates that the wallward moving vorticity in the sweep is being strongly amplified. This amplification would be expected if a vortex ring approached the wall having vorticity of the sign we have just indicated to be consistent with the sweep, because the effect of the wall, as modeled by inviscid theory, would be to stretch the ring, thus amplifying its vorticity. This amplification of vorticity in the sweep also helps us understand why, during stage one, the vorticity in the sweep, which was

of opposite sign from the mean vorticity of the layer, dominated over both that produced by the stagnation point flow and the mean flow vorticity.

During both stages one and two, it was noted that du/dx remained insignificant, suggesting that an inclined shear layer was not present during these times. However, during stages three and four we noted that du/dx increased significantly. During stage four, the average of the maximum values of du/dx is 30 per cent of the average of the maximum values of du/dy (both maximums occur close to each other). During stage three, there is a clear indication of an increase of vorticity of the same sign as the mean vorticity of the layer, occurring at the downstream end of the pocket flow module. This vorticity is presumably a redistribution of the vorticity created by the stagnation point flow due to the sweep, into a concentration that is significantly above the mean, and visually appears as a vortex in side view laser visualizations. During the time it takes the pocket pattern to evolve from stage three to stage four, the flow at $y^+ = 10$ no longer appears to be due to discrete vortices near the front of the pocket, but instead appears to be represented by a sharp shear layer. Visualizations show that the vortices still exist, generally until stage five, but have moved above the probe. This can be seen in Fig. 5. Presumably, the vorticity in the downstream portion of the sweep, and the vorticity created by the sweep's interaction with the wall, have induced each other to move upward. The juxtaposition of the vortex in the sweep which consists of high speed fluid, and the vortex created as a result of redistribution of vorticity created at the wall by the stagnation flow pattern, which consists of low speed fluid, results in the sharp shear layer. As we go from stage three to stage four, Fig. 4 also indicates that the major contribution to the Reynolds stress changes from the sweep to the ejection, which is consistent with the lifting vortices. This model also provides an explanation of the significant Reynolds stress contribution, in stages three and four, due to outward interaction events. These periods during which high speed fluid is moving away from the wall are expected to occur within the downstream sweep vortex, and as a result of the sweep vortex being induced away from the wall.

It is not yet clear how or why the lifted fluid goes rapidly turbulent as indicated in the description of stage five. The signals show that although the shear layer has disappeared, the ejection continues for some time afterwards. Furthermore, it is not clear why the stretching of the sweep vorticity does not amplify it sufficiently to overwhelm the vorticity generated downstream of the stagnation point flow, and prevent ejection of the lifted sublayer fluid, as was observed at the upstream end of the pocket

pattern. These questions require further research.

The spatial scale over which the evolution of the pocket flow module takes place can be estimated by multiplying the average convection velocity of the pocket patterns, u_{∞} , by the average duration of the pocket evolution, $t^* \approx 30$. This results in l^* on the order of 400.

V. Discussion and Comparison

A review of the literature indicates that many of the investigations into the wall region structure of turbulence have focused on events that appear to occur as part of the evolution of the pocket flow module. We will briefly point to the major correspondences, although to our knowledge even minor details of most of the investigations show close correspondence.

One of the most used hot-wire turbulence detection techniques is the one developed by Gupta, Kaplan and Laufer,²⁸ and used by Blackwelder and Kaplan,¹¹ and Blackwelder,¹² Blackwelder and Eckelmann,⁴ and many others to determine wall layer structure. The technique involves calculating a short time variance of the streamwise velocity fluctuations, averaged over an interval varying from $t^* = 15$ (Ref. 4) to $t^* = 20$ (Ref. 11). For t^* intervals of these durations, the short time averaged variance strongly resembles the du/dt signal. We have found that du/dx (obtained from du/dt using a local Taylor hypothesis) attained its largest values in the 207 boundary layer thicknesses investigated, during stage four of the pocket evolution. The only other stage where significant du/dx was found, was stage three, where the peaks were about 80 per cent as large. The average width of the peaks, measured at the signal axis, during stage four, was $t^* = 6.7$. This suggests that the detection technique is keying on the sharp shear layer developed during stage four. If a lower value of the detector function acceptance criteria is used, the signals during stage three would be included in the conditional sample. The interpretation given in Ref. 4, and 12 also suggests this. However, the scale of the pocket patterns, and hence of the pocket flow module is the order of 50-100 wall layer units, Falco and Calkins,²⁹ and depends upon Reynolds number. The suggestion in Ref. 12, that the sweep is of large scale, has come primarily from rakes of hot-wires which extend to approximately $y^* = 100$. This data shows that sharp shear layers extend out to $y^* = 0(30-50)$. Although weaker shear is sometimes apparent to the top of the rake. Our visual observations of the lifting vorticity generated by the stagnation point flow, show that, in general, it remains coherent out to $y^* = 30-50$, before breaking up (Fig. 5 shows an example in which the vortex has reached $y^* = 99$). Since the shear layer forms between this vortex and the one

in the sweep, it is clear that phenomena of the scale of delta are not directly involved. However, there is substantial evidence, Brown and Thomas,³⁰ Falco,³¹ and Chen and Blackwelder,³² that the large scale inflows are phased with the phenomena being discussed.

Blackwelder and Kaplan¹¹ show the conditionally sampled Reynolds stress pattern that results from their detection technique. Their results are shown in Fig. 6. We have inverted their signatures to enable more immediate comparison with Figures 2 and 4. We see that their signal appears to be a composite of stages three and four. It extends over roughly $t^* = 20$, has a sweep followed by an ejection, with a region of very low or negative Reynolds stress separating them. The peak averages of the sweeps in three and the ejections in stage four are similar to their values. Blackwelder and Kaplan also measured the signature $1/4$ delta downstream of the position at which their detector indicated high du/dt . They found, after correcting for the different convection velocities of individual events, the picture in Fig. 6b. This spatial separation corresponds to a temporal interval of $t^* = 8.7$, which is consistent with the time interval between stages three and four. This signature looks like that of stage four, thus indicating the same development as we have discussed for the pockets.

The pocket flow module also provides a simple explanation of the results of Blackwelder and Eckelmann⁴ which indicate that there is a change in sign of w and $dw/dy|_w$ as the sharp shear layer goes by. From Fig. 4 we expect fluid to move towards the center line of the pocket over the portion which is ejecting, while we expect movement away from the center line within the pocket pattern because the sweep is observed to cause a widening of the pattern. The narrow width of the shear layer which they measured, approximately $17 z^*$ is consistent with the half width of pockets at low Reynolds numbers (see Ref. 29). Further, the fact that after the sweep arrived we measured velocity gradient (du/dy) magnitudes larger than the mean value, is consistent with the picture during stage three of the pocket evolution, which as we have noted, would be detected by their technique.

The Lagrangian observations of the wall region made by Corino and Brodkey⁹ are also incorporated in the pocket flow module evolution. By observing events in the wall region in a data window $x^* = 63$ by $y^* = 40$ by $z^* = 20$ as they convected at a constant percentage of their pipe center line velocity, they noticed that the ejection of particles which were near the wall, resulted from the following sequence. First, a deceleration occurred within a local region near the wall. This was followed by the entrance into their field of view of a high speed region at least as

large as their data window. This high speed region interacted with the decelerated region and resulted in an ejection of fluid. Sometimes the ejection would occur just as the accelerating fluid entered the field of view, while at other times, it occurred after the acceleration process had begun. The ejection always occurred before the entire region was completely accelerated.

Fig. 4 gives, of course, the sequence of events an observer would see as he followed the flow when a pocket flow module was evolving. Fluid downstream of the pocket pattern is moving at the local mean velocity during stages 1 and 2, and is decelerated as the evolution proceeds from stage 2 to stage 3. During stage 3, the sweep moves to the downstream end of the pocket pattern, and thus it would move into the field of view of a data window located near the downstream end of the pocket pattern. It is also during stage three that we see the ejection of fluid near the downstream end of the pocket. It is important to note that the length scale of the pocket fits the Corino and Brodkey observations. Thus we see that they have also keyed upon the downstream end of the pocket flow module for a significant number of their observations. A discussion of what they would see if the side of a pocket entered their data window is given in Ref. 23.

The turbulence structure in the wall region has also been studied by Eckelmann, hychas, Brodkey and Wallace.¹³ They studied the streamwise velocity fluctuations to find a pattern that appeared to reoccur, and developed a pattern recognition program which detected the pattern in the streamwise velocity fluctuations and proceeded to store all of the other quantities they measured. The pattern consisted of a gradual deceleration from a local maximum followed by a strong acceleration. Since this description fits the pocket evolution during stages three and four, we should see some correspondence, especially in the region of the strong acceleration. Eckelmann et al measured du/dy , uv , u and v , at $y^+ = 15$, so comparisons can be made. Comparing their uv and du/dy patterns in the region of strong acceleration, with the pocket pattern during stage four, we find that both signatures are in agreement, even with respect to the phasing of du/dy and uv and u . Furthermore, the width of the du/dy peak is the same order as found in the pocket. Thus, it also appears that Ref. 13 has keyed upon the downstream end of the pocket during stages three and four. Their results which show a significant broadening and reduction in magnitude of the peak at $y^+ = 80$, reinforces this conclusion.

The pocket flow module is a flow module that integrates the sweep and ejection events, as well as the other two uv producing events. We have shown that it

is consistent with the findings of Ref. 9, and we will now show that it is consistent with the work of Offen and Kline,⁸ who studied the relationship between motions in the outer flow and the bursting process near the wall. They found that there was a close connection between sweeps found in the logarithmic region, and the bursting process indicated by wall dye. In particular, a wall-ward moving perturbation was observed in nearly every case just prior to the appearance of oscillatory motions in the wall dye. Furthermore, the oscillations at the wall are first seen downstream of the outer disturbance. This description corresponds to stage one of the pocket flow module evolution. Abstracting their results, they continue... "The wall-dye disturbances grow slowly and eventually lift up. At the same time the hydrogen bubbles (their wire was normal to the wall) show that the velocity field becomes perturbed in the region directly above the oscillating wall dye. The disturbances in the zone generally look like patterns one would expect in the presence of vortices, and these dominate the logarithmic region. Focusing attention closer to the wall, simultaneously with, or shortly after, the appearance of the wall dye perturbations, a long, narrow, high-shear zone forms just above the region of wall-dye movement. Vortices form along the apparently unstable shear line". Stage two of the pocket flow module evolution fits this description closely. The incoming sweep has moved wall dye to create the pocket pattern, and in stage two, we see that a high shear zone has formed (note du/dy) over the pocket at $y^+ = 16$. In an earlier work, Falco²³ emphasized the presence of transverse vorticity of the same sign as the mean vorticity of the layer was present along the upstream boundary of the pocket, i.e., at the end of the high shear zone noted by Offen and Kline. It is necessary to point out that the high shear zone they are referring to occurs prior to lift-up, and is different from the one associated with stages three and four of the pocket evolution described above. Continuing our abstraction of the results of Ref. 8... "most of the lift-ups of wall dye were seen some time after the formation of either a streamwise or a transverse vortex, and these began to leave the wall where the vortex came closest to the wall. The sweep generally continued to move towards the wall after the low-speed fluid element had begun to lift away from the wall... This description corresponds to stage three of the pocket flow module. At this point in the evolution, wall marker has lifted up at the upstream end and along the sides of the pockets. The vortex which lies along the boundary of the pocket is, of course, streamwise orientated along the sides. Offen and Kline had an essentially two-dimensional slice, so that they saw either a transverse vortex or a streamwise vortex. As the wall layer fluid is lifted-up, first at the back, and then progressively around the sides, the fluid

at the back wall, as it spirals along the pocket vortex, move back towards the wall and then away from it again. This would appear as the oscillation which is seen to occur after lift-up. Offen and Kline continue: "during the end of the burst's oscillatory growth stage, the interaction between the bursting fluid and the motion in the logarithmic region causes the formation of another large vortex-like structure. Some fluid from both the burst and its associated sweep, returns to the wall. When this fluid arrives at the wall, it spreads out sideways and is quickly retarded by the strong viscous forces near the wall. It is believed that this event is associated with another lift-up process farther downstream". We believe that the evolution they were describing corresponds to the end of stage three, and to stage four of the pocket evolution. During stage three, transverse vorticity of the opposite sign from that of the mean shear is amplified, and we see the start of lift-up of low speed fluid at the downstream end of the pocket pattern. The amplification of the transverse vorticity appears to be the interaction Offen and Kline note is occurring between the bursting fluid and the logarithmic region, which they suggest causes the formation of a large vortex structure. Furthermore, a high shear layer is forming at this end of the pocket pattern. In stage four, a strong ejection of sublayer fluid occurs, which as we have suggested, results from the mutual interaction of two vortices. This is the "second" ejection that Offen and Kline suggest occurs, and which is the basis of their hypothesis of the cyclic nature of the bursting process. It should be noted that they conclude their description of the bursting process by noting that breakup of the lifted sublayer fluid appears to be the result of vortices interacting, and that flow patterns in the region surrounding breakups revealed that 60 per cent of the bursts broke up immediately after an interaction with another vortical structure. During stage five of the pocket flow module evolution, we have observed breakup as the two vortices mutually interact.

Thus it appears that the description of the turbulence production process given by Offen and Kline fits that found for the pocket flow module evolution as a whole. However, their assumptions about the cyclic nature of the process now appear to be related to the lift-ups occurring first at the upstream end of the pocket pattern, and later at the downstream end. Thus, it may be that the cycle they suggest has only two lift-ups associated with it. They show that sweeps precede bursts which in turn, they suggest, interact with the log region flow to produce new sweeps further downstream. Kline³³ has noted that this statement appears to be anomalous, because the burst is, of course, low speed fluid. Our information suggests that there is one sweep associated with the pocket flow

module. The evolution of the probe signals, as well as the visual data (it should be noted that although visual indications of vorticity in sweeps have been obtained in the boundary layer, the clearest visual data relevant to this question has come from experiments with turbulent spots), indicate that the sweep is vortical, as noted by Offen and Kline, but that, furthermore, it has both forward and reversed transverse vortices in it, as seen in a streamwise light plane, or a light plane perpendicular to the flow. This strongly suggests that the vorticity of the sweep is organized into a ring. As we have noted, the evolution of our hot-wire vorticity data also supports this picture. As the sweep approaches the wall at some acute angle, one portion of this ring comes in close proximity with the wall, is stretched inviscidly, and causes the first lift-up. Then the downstream portion comes in close proximity to the wall and causes the second lift-up, which results in the strong shear and breakup. Although the pockets are found to be individual, independent flow modules, they are, however, are often found in groups (see Ref. 23). Evidence of the time for formation of members of a group of two or three pockets suggests that, in general, they form within an interval too short for one to be considered the generator of the other. However, exceptions to this have been observed.

Another interesting fact about the pocket evolution, which has been previously observed during the bursting process by Kim, Kline and Reynolds⁷ and Offen and Kline, is that the lift-ups don't continuously move outward, but instead they oscillate. The sublayer fluid which lifts up at the upstream end of the pocket, subsequently moves laterally and towards the wall and then away again, as it spirals around the vortex that exists along the boundary of the pocket pattern (hence the "oscillation"). This motion does not produce a significant uv signal at $y^+ \approx 10$ (see stage two of Fig. 4 which shows that the uv is due to the sweep). This is consistent with the findings of Offen and Kline that the breakup periods, not the lift-ups, corresponded to the times that had most of the fluctuation energy (also see Kline³³).

The recent work of Hogenes and Hanratty³⁴ which combined arrays of wall probes and hot-wires in the wall region, supports the hypothesis that the dominant flow structure is a strongly linked combination of inflows of high momentum fluid and outward flowing low momentum fluid. They found that the inflections in the velocity profile resulted from both inflows preceding outflows and outflows preceding inflows. The first sequence would occur at the upstream end of the pocket, whereas the second would occur at the downstream end.

The results of the above comparisons indicate that the probe detection technique of Ref. 29 has keyed upon the stages three and four of the pocket evolution. Corino and Brodkey have also apparently stressed this phase of the evolution. The visual data of Kim et al.⁷ and Offen and Kline⁸ have described the entire pocket evolution. As a result, the conclusion from the probe studies indicate that high speed fluid is upstream of the ejecting fluid, this was also true of the studies of Corino and Brodkey and Eckelmann et al. On the other hand, the study of Offen and Kline indicated that sweeps came to the wall downstream of the lifted-up wall layer dye, but that because of the cyclic nature of the process (as they saw it) the sweep would eventually be followed by a burst. It is now clear that the term "ejection" should be used to characterize what happens to the lifted-up wall layer dye at the end of the oscillatory growth stage, but immediately before breakup. The terms "ejection" and "lift-up" have been interchanged in the past.

Finally, we want to mention that the mechanism of the lift-ups appears to closely resemble the one studied by Voligalski and Walker.²⁰ They performed calculations of the effect of a two-dimensional vortex on the wall layer flow beneath it, when the vortex was convecting parallel to the wall in a laminar boundary layer. Downstream of the vortex, for certain combinations of vortex strength, convection velocity, and boundary layer profile shape, a stagnation type flow pattern existed near the wall, which resulted in creation of vorticity (Ref. 2b). The influence of the original vortex on this newly created vorticity, which is of opposite sign, is to induce it off the wall, resulting in lift-up. It appears to be the mechanism operational around the boundary of the pocket. However, it fails to result in the ejection of fluid lifted-up in the upstream portion of a pocket because vortex stretching has made the sweep vortex much stronger, as noted above. Of course, vortex stretching can't occur in two-dimensional flows. The mechanism is effective at the downstream end of a pocket, because stretching of the sweep vortex has apparently ceased. Here, the vortices mutually induce themselves to the log region before breakup occurs.

Summary and Conclusions

Simultaneous multi-probe hot-wire data and flow visualization experiments have shown that a flow module exists which is responsible for a large fraction of the Reynolds stress and shear measured in the wall region. Its scale is on the order of 100 wall layer units, and its period of occurrence is the same as that measured for ejections of sublayer fluid. The flow module evolves from a vortical sweep into an ejection which breaks down into both smaller and larger scales, in t^+ on the

order of 30. The mechanisms involved include; stretching of the vorticity in the sweep, the generation of vorticity near the wall by the stagnation point flow that the sweep creates, mutual interaction of the vortices formed as a result of these processes leading to motion away from the wall. The distinct pocket pattern results because the sweep vortex is amplified to the extent that it induces the stagnation flow generated vortex around itself. This lift-up of sublayer fluid results in a pair of short streaks which appear to oscillate as the lifted-up fluid is returned back towards the wall. When the front of the sweep reaches the wall, the sweep vortex and the stagnation flow generated vortex do induce each other out to the log region. In doing so, a sharp shear layer is created between the two vortices. By the time they get out to $y^+ = 30-50$, they breakup. It is not clear why the stretching of the sweep's ring vortex ceases before its vorticity is diffused, allowing this outward ejection.

Thus, the formation of streamwise and transverse vorticity concentrations of short duration, intermediate scale streaky structure, the sudden lift-ups, the oscillations, and the breakup, are seen to be phased to the stages of evolution of this flow module.

Acknowledgements

This work was jointly sponsored by the Office of Naval Research, Fluid Dynamics Branch, and by the Air Force Office of Scientific Research. Their financial assistance is greatly appreciated.

References

- 1 Townsend, A. A., "The Structure of Turbulent Shear Flows" Cambridge University Press, Cambridge, U. K., 1976.
- 2 Bakewell, H. P. and Lumley, J. L., "Viscous Sublayer and Adjacent Wall Region in Turbulent Pipe Flow," *Physics of Fluids*, Vol. 10, 1967, p. 1880.
- 3 Lee, M. K., Eckelmann, L. D., and Hanratty, T. J., "Identification of Turbulent Wall Eddies Through the Phase Relation of the Components of the Fluctuating Velocity Gradient," *Journal of Fluid Mechanics*, Vol. 66, 1974, pp. 17-33.
- 4 Blackwelder, R. F. and Eckelmann, H., "Streamwise Vortices Associated with the Bursting Phenomenon," *Journal of Fluid Mechanics*, Vol. 94, 1979, pp. 577-594.
- 5 Kundstadler, P. W., Kline, S. J., and Reynolds, W. C., "An Experimental Investigation of the Flow Structure of the Turbulent Boundary Layer," Report MD-8, Dept. of Mech. Engrg., Stanford Univ., Stanford, CA., 1963.
- 6 Schnaub, F. A. and Kline, S. J., "A Study of the Structure of the Turbulent Boundary Layer with and without Longitudinal Pressure Gradients," Report MD-12, Dept. of Mech. Engrg., Stanford Univ., Stanford, CA., 1965.

- 7 Kline, H. T., Kline, S. J., and Reynolds, W. C., "An experimental Study of Turbulence Production Near a Smooth Wall in a Turbulent boundary Layer with Zero Pressure Gradient," Report MD-20, Dept. of Mech. Engrg., Stanford Univ., Stanford, CA., 1966.
- 8 Offen, G. H., and Kline, S. J., "Experiments on the Velocity Characteristics of 'bursts' and on the Interactions between the Inner and Outer Regions of a Turbulent Boundary Layer," Report MD-31, Dept. of Mech. Engrg., Stanford Univ., Stanford, CA., 1973.
- 9 Corino, E. M. and Brodkey, R. S., "A Visual Investigation of the Wall Region in Turbulent Flow," Journal of Fluid Mechanics, Vol. 37, 1969, pp. 1-30.
- 10 Grass, A. J., "Structural Features of Turbulent Flow Over Smooth and Rough boundaries," Journal of Fluid Mechanics, Vol. 50, 1971, pp. 233-254.
- 11 Blackwelder, R. F. and Kaplan, R. E., "On the Bursting Phenomena Near the wall in Bounded Turbulent Shear Flows," Journal of Fluid Mechanics, Vol. 76, 1976, pp. 89-112.
- 12 Blackwelder, R. F., "The Bursting Process in Turbulent Boundary Layers," Coherent Structure of Turbulent Boundary Layers, ed. C. R. Smith and D. E. Abbott, AFOSR/Lehigh, 1978, pp. 48-94.
- 13 Eckelmann, H., Nychas, S. G., Brodkey, R. S., and Wallace, J. M., "Vorticity and Turbulence Production in Pattern Recognized Turbulent flow Structures," Physics of fluids, Vol. 20, Part II, 1977, pp. S225-S231.
- 14 Praturi, A. K. and Brodkey, R. S., "A Stereoscopic Visual Study of Coherent Structures in Turbulent Shear Flow," Journal of Fluid Mechanics, Vol. 89, 1978, pp. 251-272.
- 15 Landahl, M. T., "Modeling of Coherent Structure in Boundary Layer Turbulence," Coherent Structure in Turbulent Boundary Layers, ed. C. R. Smith and D. E. Abbott, AFOSR/Lehigh, 1978, pp. 340-364.
- 16 Theodorsen, T., "Mechanism of turbulence," Proc. of 2nd Midwestern Conf. Fluid Mech., The Ohio State Univ., Columbus, Ohio., 1952, p. 1.
- 17 Willmarth, W. W. and Tu, B. J., "Structure of Turbulence in the Boundary Layer near the wall," Physics of Fluids, Supplement to Vol. 10, 1967, pp. S134-S137.
- 18 Kline, S. J., Reynolds, W. C., Schraub, F. A., and Kunstadler, P. W., "The Structure of Turbulent Boundary Layers," Journal of Fluid Mechanics, Vol. 30, 1967, pp. 741-774.
- 19 Nychas, S. G., Hershey, H. C., and Brodkey, R. S., "A Visual Study of Turbulent Shear Flow," Journal of Fluid Mechanics, Vol. 61, 1973, pp. 513-525.
- 20 Doligalski, T. L. and Walker, J. D. A., "Shear Layer Breakdown due to Vortex motion," Coherent Structure in Turbulent boundary Layers, ed. C. R. Smith and D. E. Abbott, AFOSR/Lehigh, 1978, pp. 288-332.
- 21 Falco, R. E., "Wall Layer Structure of Turbulent Boundary Layers," Bulletin Am. Physical Society, Series II, Vol. 23, 1978, p. 1000.
- 22 Falco, R. E., "A Structural Model of the Turbulent Boundary Layer," Proceedings of the 14th Annual Meeting of Society of Engineering Sciences, 1977.
- 23 Falco, R. E., "Structural Aspects of Turbulence in Boundary Layer Flows," to be published in the Proceedings of the Sixth Biennial Symposium on Turbulence, 1979.
- 24 Falco, R. E., "The Role of Outer Flow Coherent Motions in the Production of Turbulence Near a Wall," Coherent Structure of Turbulent Boundary Layers, ed. C. R. Smith and D. E. Abbott, AFOSR/Lehigh, 1978, pp. 448-461.
- 25 Falco, R. E., "Combined Simultaneous Flow Visualization/Hot-Wire Anemometry for the Study of Turbulent Flows," ASME Journal of fluids Engineering, Vol. , 1980.
- 26 Wallace, J. M., Eckelmann, H., and Brodkey, R. S., "The wall Region in a Turbulent Shear Flow," Journal of Fluid Mechanics, Vol. 54, 1972, pp. 39-48.
- 27 Comte-Bellot, G., Sabot, J., and Salen, L., "Detection of Intermittent Events Maintaining Reynolds Stress," Proceedings of the Dynamic Flow Conference, 1978, pp. 213-229.
- 28 Lighthill, M. J., "Introduction. Boundary Layer Theory," in Laminar Boundary Layers, ed. L. Rosenhead, Oxford University Press, 1963, pp. 46-102.
- 29 Gupta, A. K., Laufer, J., and Kaplan, R. E., "Spatial Structure in the Viscous Sublayer," Journal of Fluid Mechanics, Vol. 50, 1971, pp. 493-512.
- 30 Falco, R. E. and Calkins, J., "Transverse Vorticity Measurements in Turbulent boundary Layers," Bulletin Am. Physical Society, Series II, Vol. 24, 1979, p. 1132.
- 31 Brown, G. L. and Thomas, S. W., "Large Structure in a Turbulent Boundary Layer," Physics of Fluids, Vol. 20, Part II, 1977, pp. S243-S252.
- 32 Falco, R. E., "Coherent Motions in the Outer Region of Turbulent Boundary Layers," Physics of Fluids, Vol. 20, Part II, 1977, pp. S124-S132.
- 33 Chen, C. P. and Blackwelder, R. F., "Large-Scale Motion in a Turbulent boundary Layer: A Study Using Temperature Contamination," Journal of Fluid Mechanics, Vol. 89, 1978, pp. 1-31.
- 34 Kline, S. J., "The Role of Visualization in the Study of the Structure of the Turbulent Boundary Layer," Coherent Structure of Turbulent Boundary Layers, ed. C. R. Smith and D. E. Abbott, AFOSR/Lehigh, 1978, pp. 1-26.
- 35 Hogenes, J. M. A. and Hanratty, T. J., "Identification of the Dominant Flow Structure in the Viscous wall Region of a Turbulent Flow," Report 2, Dept. of Chemical Engrg., Univ. of Illinois, Urbana, 1979.

Source	$T_B U_\infty / \nu$	comments
Blackwelder and Kaplan ($R_\theta = 2550$)	10	hot-wire
Offen and Kline ($R_\theta = 820$)	5 10	ejections bursts (dye)
Schraub and Kline ($R_\theta = 1000-1700$)	4.5-5.5	H ₂ bubbles
Ueda and Hinze ($R_\theta = 11,450, 35,500$)	4.7	hot-wire
Willmarth and Lu ($R_\theta = 4320$)	4	hot-wire
Present Work ($R_\theta = 1350$)	5	pockets

Table 1. Comparison of average times between bursts and the passage of pocket flow modules in the turbulent boundary layer.

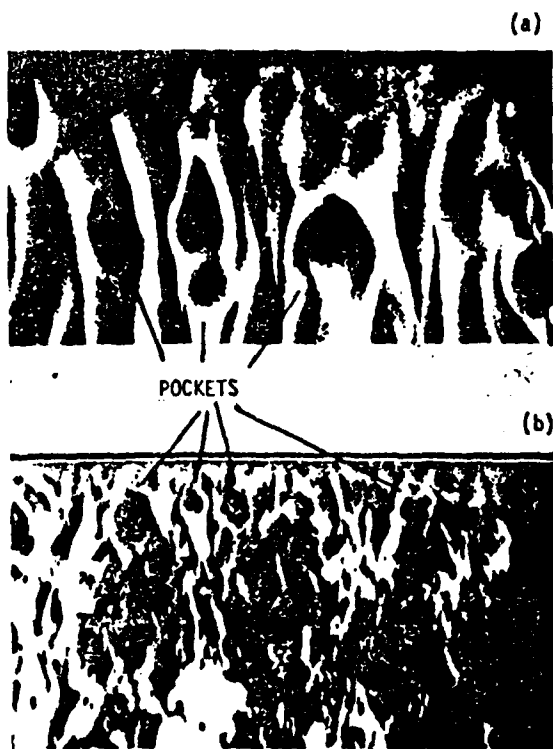


Fig. 1. Pockets revealed by oozing oil-fog contaminant through a slit in the wall under a turbulent boundary layer. The flow is from top to bottom, and the slit is located close to the top of each photograph. (a) $R_\theta = 738$; (b) $R_\theta = 2745$.

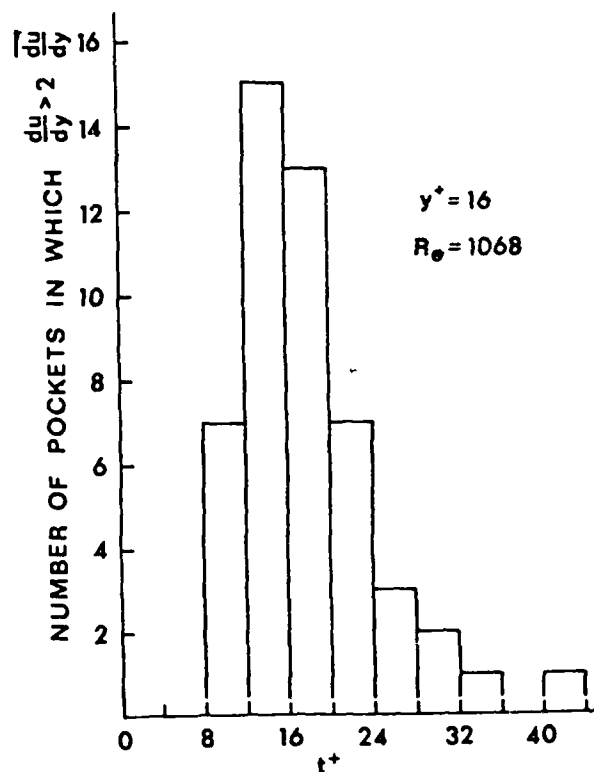


Fig. 3. The distribution of pockets in which du/dy was greater than $2du/dy$, vs the age of the pocket when it contacted the probe, which was a $y^+ = 16$.

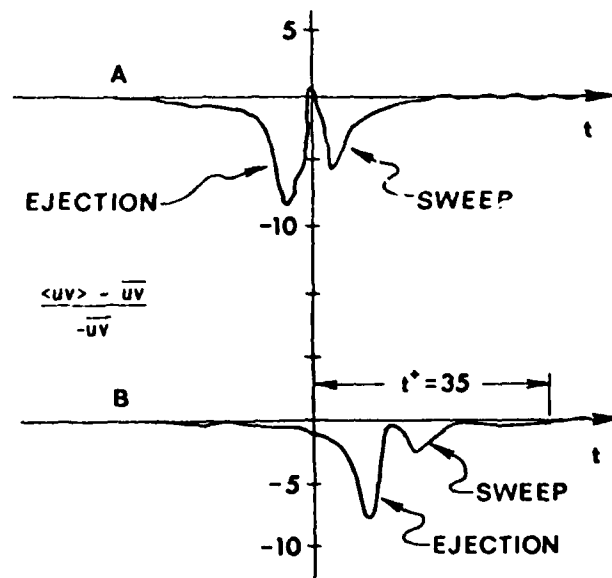


Fig. 6. Conditional averages of the Reynolds shear stress at $y^+ = 15$, after Blackwelder and Kaplan, Ref. 11. (a) Detector function at sampling position. (b) Sampling probe $1/4 \delta$ downstream ($\Delta t = 8.7$) of the detector probe. The earlier peak is due to ejections, while the later one is due to sweeps. Note how the sweep decays while the ejection persists (see text for a discussion of comparison with Fig. 4).

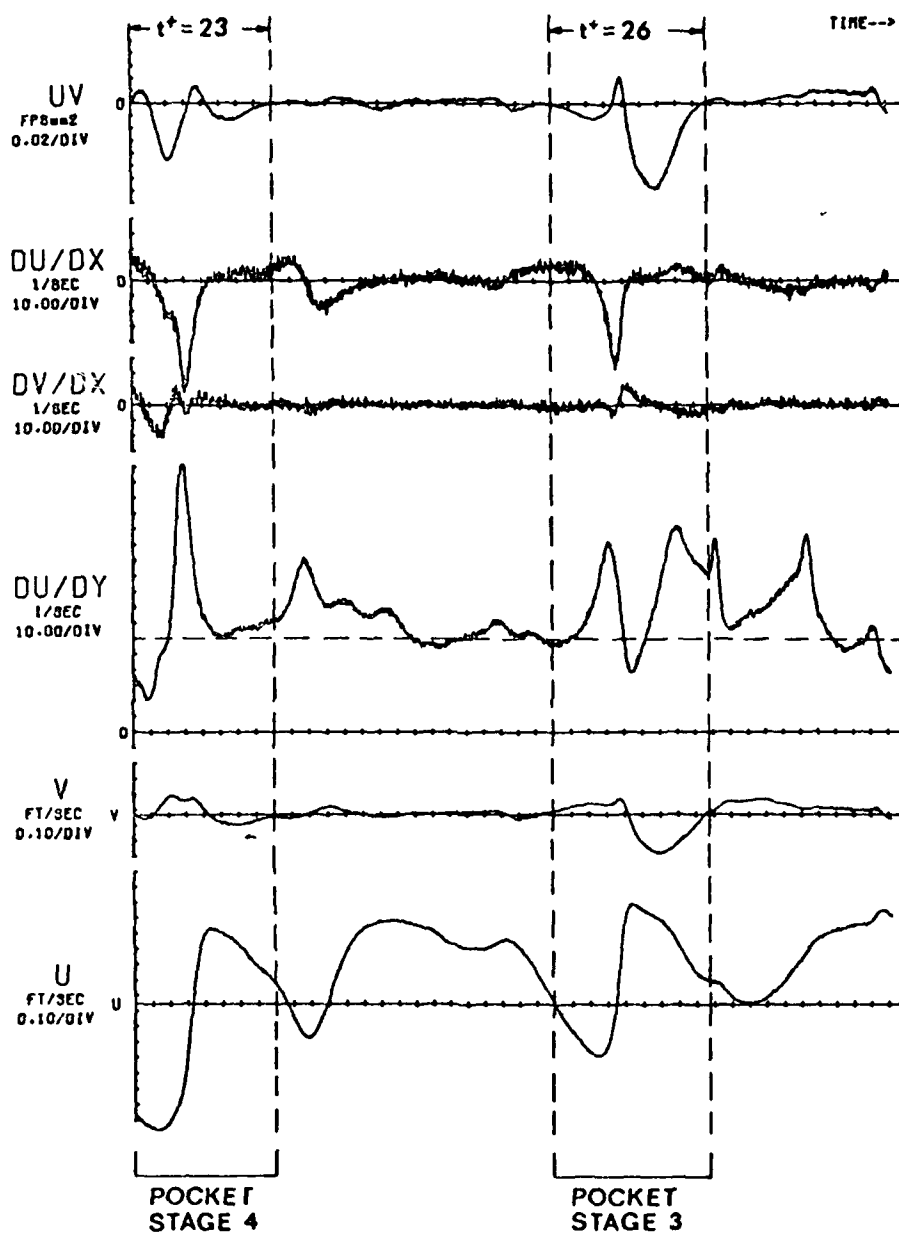


Fig. 2. Simultaneous records of uv , du/dx , dv/dx , du/dy , v , and u at $y^* = 16$ in a turbulent boundary layer. The dashed vertical lines bound pocket flow modules. The first pocket passes the probe during stage four of its evolution, while the one which arrives later in in stage three of its evolution. The dashed line on the du/dy signal is the mean shear. $R_\theta = 1060$.

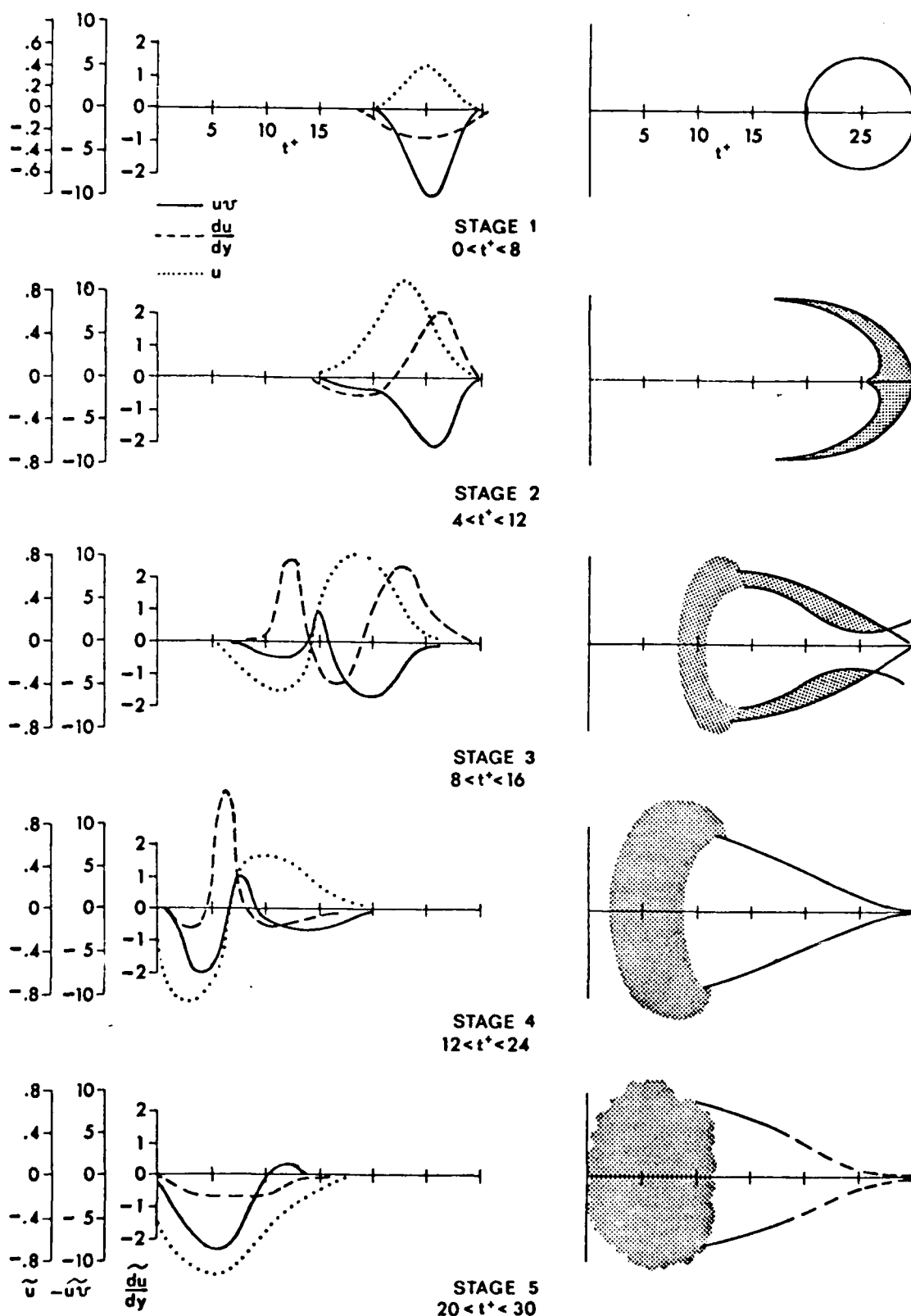


Fig. 4. The evolution of the pocket flow module. The plan view pocket patterns and the ensemble averaged signatures of u , uv , and $\frac{du}{dy}$ for each of five stages, are shown. In the visual patterns, shading indicates lifted fluid. The signals, measured at $y = 16$, indicate conditions along the centerline of the pocket. The visual and hot-wire data have the same abscissa, and the placement of the signals is phased with the visual pattern, both within each stage and between stages. The ordinates correspond to $(\langle u \rangle - \bar{u})/\bar{u}$, $(\langle uv \rangle - \bar{uv})/\bar{uv}$, and $(\frac{du}{dy} - \bar{\frac{du}{dy}})/(\bar{\frac{du}{dy}})$. The stages are arranged to show the development an observer would see if he moved with the speed of the upstream end of the visual pattern.

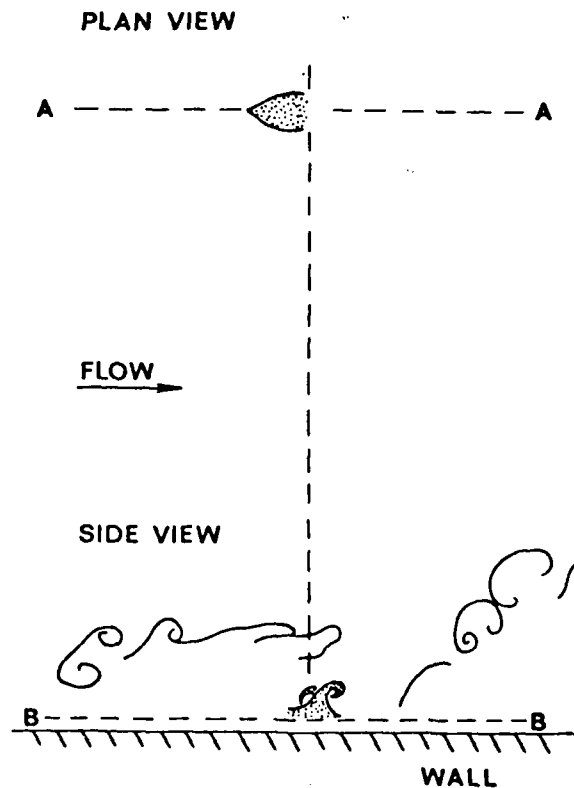


Fig. 5. Simultaneous views of the buffer layer of a smoke marked turbulent boundary layer (top, plan view), and of a slice of the layer normal to the wall above it. Line A-A of the accompanying sketch represents the edge of the light plane which illuminates the side view. Line B-B represents the edge of the light plane which illuminates the plan view. A pocket which is in stage four of its evolution, can be seen in the plan view (note shaded features in sketch) centered over the vertical light sheet. In the side view we can see the ejected vortex and the remains of the sweep vortex (see text).

EN
DAT